Optimizing the valorization of industrial by-products for the induction healing of asphalt mixtures

Vila-Cortavitarte, Marta; Jato-Espino, Daniel; Tabakovic, Amir; Castro-Fresno, Daniel

DOI
10.1016/j.conbuildmat.2019.116715

Publication date
2019

Document Version
Accepted author manuscript

Published in
Construction and Building Materials

Citation (APA)
Vila-Cortavitarte, M., Jato-Espino, D., Tabakovic, A., & Castro-Fresno, D. (2019). Optimizing the valorization of industrial by-products for the induction healing of asphalt mixtures. *Construction and Building Materials*, *228*, Article 116715. https://doi.org/10.1016/j.conbuildmat.2019.116715

Optimizing the valorization of industrial by-products for the induction healing of asphalt mixtures

Marta Vila-Cortavitarte[1,*]; Daniel Jato-Espino[1]; Amir Tabakovic[2,3,4] ; Daniel Castro-Fresno[1]

[1] GITECO Research Group, Universidad de Cantabria, Av. de los Castros 44, 39005, Santander, Spain
[2] Research Enterprise and Innovation Services, Technological University Dublin, Dublin, Ireland
[3] School of Civil Engineering, University College Dublin, Dublin, Ireland
[4] Microlab, Faculty of Civil Engineering and Geosciences, Delft University of Technology, Delft, The Netherlands.

** Corresponding author. E-mail address: marta.vila@unican.es; Tel.: +34 942203943; Fax: +34 942201703*

Abstract Self-healing within asphalt pavements is the process whereby road cracks can be repaired automatically when thermal and mechanical conditions are met. To accelerate and improve this healing process, metal particles are added to asphalt mixtures. However, thisapproach is costly both in economic and environmental terms due to the use of virgin metallic particles. So, even though the self-healing of asphalt mixtures has been widely addressed in experimental terms over the years, there is a lack of research aimed at modelling this phenomenon, especially with the purpose of optimizing the use of metal particles through the valorization of industrial by-products. As such, the goal of this study was to develop a statistical methodology to model the healing capacity of asphalt concrete mixtures (AC-16) from the characteristics of the metal particles added and the time and intensity used for magnetic induction. Five metal particles were used as heating inductors, including four types of industrial by-products aimed at transforming waste products into material for use in the road sector. The proposed approach consisted of a combination of cluster algorithms, multiple regression analysis and response optimization, which were applied to model laboratory data obtained after testing asphalt concrete mixtures containing these inductors. The results proved the accuracy of the statistical methods used to reproduce the experimental behaviour of the asphalt mixtures, which enabled the authors to determine the optimal amount of industrial by-products and time needed to make the self-healing process as efficient as possible.

Keywords Asphalt mixtures; Cluster analysis; Industrial by-products; Multiple regression analysis; Response optimization; Self-healing; Waste Valorisation.

1. Introduction

Self-healing technology has revolutionized the design, construction and maintenance of asphalt pavements, and can have great economic and environmental effects on the construction industry. The most efficient self-healing concept for asphalt pavements, is induction healing. Induction healing allows asphalt pavements to repair within 3 minutes of exposure to induction heating. However, the main drawback to this induction aided self-healing approach is the amount of metal particles required in the asphalt mixtures to enable efficient and effective asphalt repair [1].

To achieve induction healing, the amount of metal particles usually added to asphalt mixtures is 5-10% of the bitumen [2–4], which translates into 0.28-0.55% of steel particles in the mixture. Currently, steel fibre costs €855-873 per tonne, a value which is expected to increase in the future due to the growing demand for steel from the construction industry. The average cost of asphalt in the EU is €562 per ton [5]. If steel is added to asphalt mixtures in a percentage of 0.28-0.55%, the cost of asphalt mixtures per tonne would increase by between 50-100%. As such, these economic considerations make the adoption of this technology unaffordable for the road owners in the asphalt industry.

However, in line with previous studies on the incorporation of waste materials into asphalt pavements for different purposes [6–8], recent investigations have explored the use of metal by-products as a means of improving the resource and recycling efficiency of the self-healing process [4,9–11]. Research on self-healing for asphalt pavements have primarily focused on the experimental characterization of the healing capacity of asphalt concrete [12–14], porous asphalt [4,15,16] and stone mastic asphalt [17] mixtures through the addition of virgin metal particles.

A few studies have addressed the numerical modelling of asphalt self- healing using either mechanistic or discrete approaches. Qiu et al. [18] developed a cohesive zone model based on non-linear fracture mechanics with the support of finite element code to reproduce a monotonic loading-healing-reloading procedure. Although modelling and experimental results were in acceptable agreement, they differed from each other in terms of long-term displacement. Magnanimo et al. [19] used a discrete element method to model the macroscopic self-healing response of asphalt mixtures when subject to uniaxial compression (tension) tests [20]. Again, the model captured the basic behaviour of asphalt mixtures; but they recommended further research into their strain-rate dependence. Yang et al. [21] applied the discrete element method to simulate the fracture strength recovery ratio of single-edge notched asphalt mixtures after induction healing. Their simulated results qualitatively matched the experimental tests in terms of peak load and slope of load increase.

Other authors have approached the healing of asphalt mixtures as their recovery capacity during mechanical tests. Chowdary and Murali Krishnan [22] tested the accuracy of a constitutive modelling framework to replicate healing experiments carried out through repeated triaxial tests. Luo et al. [23] used an energy-based mechanistic approach

to characterize the decrease of damage density during the healing process of asphalt mixtures based on a step-loading recovery test. Levenberg [24] formulated a non-linear viscoelastic constitutive model to simulate the healing capacity of asphalt concrete during recovery intervals of uniaxial compression and standard complex modulus experiments. They all reached a satisfactory graphical fit to their laboratory results.

All of these investigations assess the 'goodness-of-fit' of their models qualitatively, in other words, they lack any numeric measure to guarantee the validity of the simulated results. Moreover, some of these studies highlighted the complexity of modelling asphalt mixtures through numerical methods, due to their shape, size, distribution of aggregates and air voids or chemistry [22], while others highlighted the optimization of the healing process as an important step to ensure durable asphalt pavements [18].

As a result of these considerations, a research gap was identified in relation to the development of a simpler and more accurate method of optimising the self-healing behaviour of asphalt mixtures. In comparison with numerical approaches, statistical methods provide a more accessible means of modelling physical phenomena through the mathematical combination of a set of contributing factors, with the added value of their capacity of testing significance hypotheses to verify the validity of the results achieved. Hence, this study aimed at designing a statistical framework to model the healing capacity of asphalt concrete mixtures, enabling the prediction of either the amount of metal particles or the heating time needed for achieving a certain road repair performance, depending on the preferences of the decision-makers. The underlying objective is the valorisation of metal waste through the optimization of the self-healing process in asphalt mixtures in terms of either resource or time efficiency.

2. Methodology

The proposed framework was intended to facilitate the modelling of the healing potential of asphalt mixtures containing metal additives as heating inductors, based on the coupling of experimental and statistical methods. A series of laboratory tests were designed in the first instance to enable the characterization of both metal particles and asphalt mixtures in terms of healing capacity. The experimental results were then modelled using a combination of statistical techniques including cluster analysis, regression analysis and response optimization.

2.1. Experimental Setup

The laboratory work focused on the determination of the Healing Ratio (HR) of asphalt mixtures. HR is a measure that compares the strength of an asphalt mixture before and after a three point bending test [3]. All of the steps required to calculate HR, shown in Figure 1, are explained in detail below.

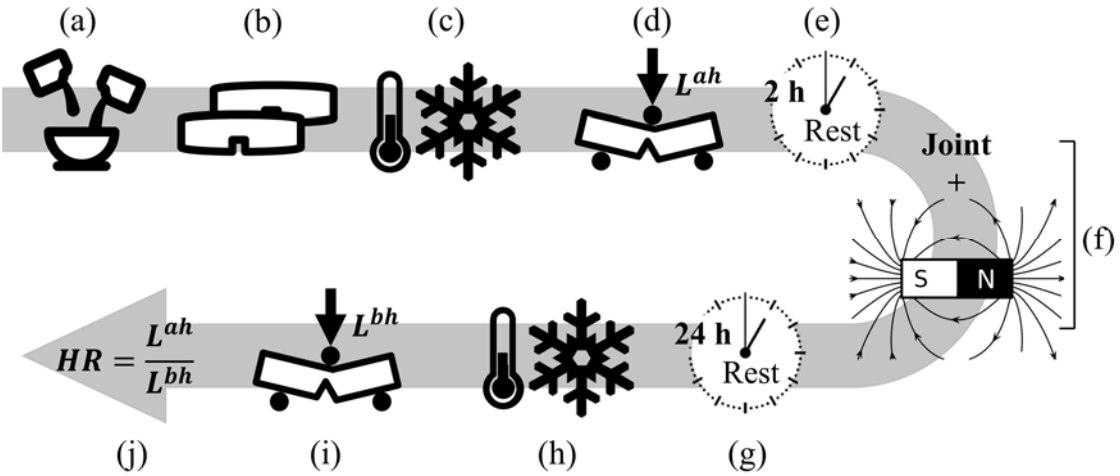

Figure 1. Flowchart of the experimental steps (a to j) conducted in laboratory to determine the healing ratio (*HR*) of asphalt mixtures: (a) mixture dosage, (b) specimen manufacturing, (c) and (h) cooling-down times, (d) breaking test after healing, (e) and (g) rest period times, (f) specimen joint and magnetic induction, (h) three point bending test before healing and (j) *HR* calculation.

The first stage (Figure 1(a)) was the dosage of asphalt mixtures, which consisted of the following components: ophite stone as coarse aggregate and limestone as fine aggregate (from 0.063 mm to 2 mm), conventional bitumen 50/70 and metal particles of different nature to enable the healing process under magnetic induction. Up to 5 different mixtures were studied by only changing this last component and then adjusting the dosage to fit the particle size distribution of a dense asphalt mixture (AC-16), as depicted in Figure 2. To this end, both the particle size distribution (UNE 933-1) [25] and the specific weight (kg/m^3) of the mixtures were calculated through the pycnometer method following the UNE 1097-4 [26] standard.

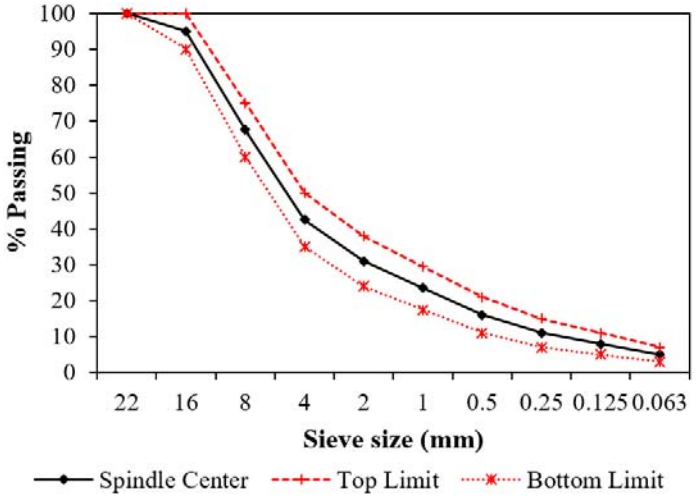

Figure 2. Particle size distribution of a dense asphalt concrete mixture (AC-16)

The materials used as metal particles, which are shown in Figure 3, included virgin steel grits (VM), by-products from blasting processes in the form of steel spheres (SBP) and grits (GBP), dust by-products filtered from blasting processes (FBP) and green slags from metal manufacturing (GSBP). In all cases, they were waste materials from metal manufacturing processes. As such, they are potentially a valuable resource that can be used in the design and production of asphalt mixtures to improve the healing process in economic and environmental terms. These by-products were used as heating inductors and/or supplementary aggregates either in isolation or in combination with each other. Their heating capacity was measured by testing them under magnetic induction and registering the temperature they achieved, if any, using a thermal camera.

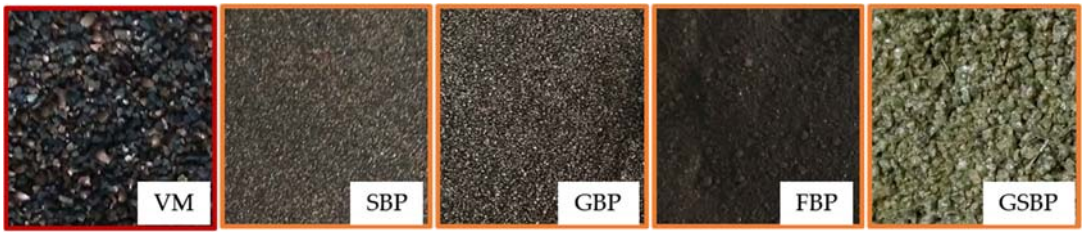

Figure 3. Metal Particles used in the study

The next step, represented in Figure 1(b), was the manufacturing of the mixtures, in which ferromagnetic particles were added together with the fine aggregates. The distribution of these particles into the specimens was assumed to be uniform, since no formation of clusters was observed during their mixing. The sample size corresponded to half-height Marshall specimens, which were compacted by 40 blows each side using an impact compactor [11]. The reduced dimensions of the specimens were chosen with the aim of saving resources, in line with the recycling aim of the research. After de-molding the specimens, they were pre-notched with a saw to produce a straight crack. Then, the specimens were stored in a freezer for 24 hours, in order to ensure that the straight crack remained unaltered when breaking (Figure 1(c)). In addition to experimental mixtures manufactured using the by-products shown in Figure 3, a control asphalt mixture containing fresh steel grits was designed due to the innate ferromagnetic behaviour of these particles.

Once the specimens were frozen, the breaking test (three point bending test as shown in Figure 1(d)) was conducted using an ad-hoc manufactured cradle with a 7 cm separation between supports, as shown in Figure 4(a). This test yielded the max load resistance by the mixtures before healing (L^{bh}), which was the first parameter to include in the equation to obtain HR. This load was recorded by a cell inserted into the compression machine.

After the initial test (break), the specimens were left to rest for two hours (Figure 1(e)), in a temperature controlled room (20ºC) before the sixth and more complex stage, the healing (Figure 1(f)). The healing was carried out using the magnetic induction using an EASYHEAT machine (Figure 4(b)). The frequency of the test was set at 329 Hz, whilst

the values of intensity and time used varied between 200 A and 600 A and 90 s and 300 s, respectively. The temperature achievements during each test were recorded by an Optical Pris Thermal camera, as shown in Figure 4(c).

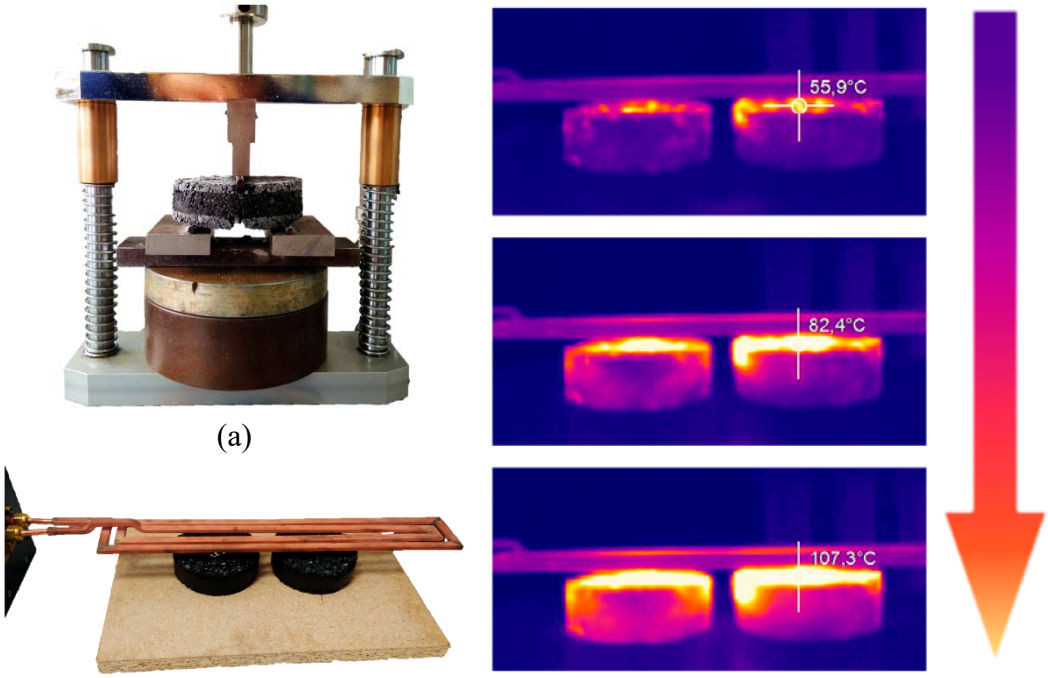

Figure 4. Details of the break-heal-break test (a) Ad-hoc cradle manufactured to support the three-point bending test (b) Position of the specimens under the coil during magnetic induction (c) Thermographic images of the specimens when being increasingly heated

The penultimate phase consisted of letting the specimens rest for 24 hours before repeating the 24 hours freezing and then breaking them through the three-point bending test previously described (Figures 1(g) and (h)). The second test (break) shown in Figure 1(i) involved obtaining the load resisted by the specimens after healing (L^{ah}), which allowed the calculation of HR using Eq (1). Taking into account that the geometric characteristics of the specimens were the same before and after healing, it can be assumed that the ratios among the loads recorded before and after healing were the same that those corresponding to the values of resistance achieved, as illustrated in Figure 1(j).

$$HR = \frac{L^{ah}}{L^{bh}} = \frac{R_t^{ah}}{R_t^{bh}} \quad (1)$$

2.2. Statistical modelling

2.2.1. Cluster Analysis

Cluster analysis is a term coined by Tryon in 1939 [27], who defined it as a set of algorithms devoted to group different elements based on their similarity to each other. In terms of this research, this technique enabled the partition of the initial types of asphalt mixtures into a series of groups or clusters. According to the main premise of cluster analysis, this implied that the specimens contained in the same group were alike, whilst they differed from the mixtures belonging to other clusters.

The particular approach selected for this purpose was bottom-up hierarchical clustering. Unlike k-means clustering, this process does not require an aprioristic notion of the desired number of clusters and involves fewer assumptions regarding the distribution of the data. Its working principle consists of allocating a cluster to each item and then start a repetitive procedure whereby the items are combined in larger and increasingly heterogeneous clusters according to their similarity, until they all are grouped into a single conglomerate [28].

Since hierarchical clustering is based on arranging the data as a distance matrix, the number of groups to choose is determined by the similarity measure and linkage method used. In this case, the Euclidean distance was selected as a similarity measure, since it is one of the most adequate alternatives to deal with interval data [29]. The formulation corresponding to this measure is provided in Eq. (2).

$$d_{ij} = \sqrt{\sum_{k} \left(x_{ik} - x_{jk}\right)^2} \tag{2}$$

where d_{ij} is the distance between items i and j, such that x_{ik} and x_{jk} represent their values across the k variables included in the analysis. As for the clustering algorithm, the approach taken was complete linkage, also known as the farthest neighbour method. In comparison with other hierarchical clustering techniques, this was the method proving to be less sensitive to identify false clusters [30]. The distance between two clusters is computed according to the maximum separation between the members within them, as expressed in Eq. (3).

$$D_{mk} = \max\left(D_{ik}, D_{jk}\right) \tag{3}$$

where $D_{c_1c_3}$ is the distance between clusters c_1 and c_3, $D_{c_2c_3}$ is the distance between clusters c_2 and c_3 and D_{mc_3} is the distance between clusters m and c_3, such that m is the merged conglomerate containing clusters c_1 and c_2. Both distances and clusters are calculated based on the values achieved by the items to compare across more than two variables. In this case, asphalt mixtures were clustered according to the density and content of their metal particles, which represented the intrinsic properties of the heating inductors used.

The interpretation of the output yielded by cluster analysis is supported with a dendrogram, which is a tree plot indicating how the items are grouped into larger clusters progressively. To this end, it measures the similarity level between the clusters at each step of the process, facilitating the decision on where to cut it and determine the final grouping.

2.2.2. Multiple Regression Analysis

The predictive modelling of the self-healing capacity of asphalt mixtures was approached using Multiple Regression Analysis (MRA), which enabled exploring the relationships between HR, which was the response to fit (Y), and a series of variables involved in the induction heating process, which served as predictors (X_i, X_j).

In particular, the predictors considered included the specific weight (X_1, kg/m^3) and content (X_2, %) of metal particles, as well as the time (X_3, s) and intensity (X_4, A) set for the application of induction heating. The type of bitumen was not considered as a predictor because it was the same in all the mixtures, whilst heating temperature was only recorded at the surface of the specimens and, therefore, lacked enough representativeness. Since the proposed variables were assumed to interact to each other, the MRA model was expressed as shown in Eq. (4).

$$Y = B_0 + \sum_{i=1}^{n}\sum_{j=1}^{n} B_{ij} * X_i * X_j + E \quad (4)$$

where B_0 is the constant of the regression equation, B_{ij} refers to the coefficients by which the predictors are multiplied and E represents the residuals derived from the regression. This model was built according to a significance level of 0.05 [31], such that those terms demonstrating to be above that threshold were discarded for subsequent steps. To ensure the pertinence of the terms included in MRA, their Variance Inflation Factors (VIF) were determined to prevent any multicollinearity effect.

The quality of the model was assessed using two main goodness-of-fit measures: the standard error of the regression (S) and the predicted coefficient of determination (pred. R^2). S indicates the distance between the observed and fitted values taken by the response, whilst pred. R^2 involves an evolution of the standard (R^2) and adjusted (adj. R^2) coefficients of determination. It is calculated by systematically removing each observation from the model and then calculating how well the omitted values are predicted.

In addition to these general verifications, the validity of the regression model was verified through a residual analysis. This consisted of evaluating the distribution of E in terms of normality [32], homoscedasticity [33] and independence [34,35], thus preventing

the existence of type I and type II errors [36]. Table 1 compiles the graphical and analytical tests undertaken to test these assumptions.

Table 1. Graphical and analytical tests used to check the assumptions related to residual analysis

Assumption	Verification	
	Graphical	**Analytical**
Normality	Quantile-Quantile plot / Histogram	Ryan- Joiner test
Homoscedasticity	Standardized residual vs Fitted value plot	Levene's test
Independence	Standardized residual vs Observation order plot	Durbin-Watson statistic

2.2.3. Response Optimization

In the context of this investigation, response optimization was used to determine the combination of factors leading to achieve a target value of HR, based on the MRA model built in the previous step. This was accomplished using the desirability function approach, which enables evaluating how well a combination of settings satisfies the purpose sought by the response. In other words, response optimization was provided by the combination of factors that best fitted the healing ratio desired for the mixtures, with the restriction that the values obtained must remain within their upper and lower bounds.

Since there was only one response to optimize (HR), the approach taken was limited to the individual desirability (δ_i) of the settings established to target a fitted response value $\hat{Y}_i$. $\delta_i(\hat{Y}_i)$ ranges from 0 to 1, such that 1 represents an ideal solution. Eq. (5) formulates the desirability function proposed by Derringer and Suich (1980) [37] to calculate $\delta_i(\hat{Y}_i)$ when the response is target-based.

$$\delta_i(\hat{Y}_i) = \begin{cases} 0, & if\ \hat{Y}_i < L_i \\ \left(\dfrac{\hat{Y}_i - L_i}{T_i - L_i}\right)^s, & if\ L_i \le \hat{Y}_i \le T_i \\ \left(\dfrac{\hat{Y}_i - L_i}{T_i - L_i}\right)^t, & if\ T_i \le \hat{Y}_i \le U_i \\ 0, & if\ \hat{Y}_i > U_i \end{cases} \quad (5)$$

where L_i, U_i and T_i are the lower, upper and target values desired for the response, whilst s and t represent how important is to achieve the target value. Hence, $\delta_i(\hat{Y}_i)$ increases linearly towards T_i in case $s = t = 1$, whereas the function becomes convex and concave if $s < 1,\ t < 1$ and $s > 1,\ t > 1$, respectively.

Given the values of specific weight and intensity of the metal particles to be modelled, the application of response optimization was aimed at fitting the values of HR targeted by making variations in the content of inductors and heating time, depending on whether resource efficiency or quickness are a priority. These variations were restricted by the

maximum and minimum values of specific weight and intensity in the mixtures considered, which performed as constraints in the optimization problem. Variation were detected among the collected data.

3. Results and discussion

This section displays and examines the main results obtained through the application of the experimental and statistical approaches described in the methodology. To ensure the cohesion between both sections, the results are presented according to the same structure used above, whereby the experimental outputs lay the foundations required for the statistical analyses.

3.1. Experimental Setup

Figure 5 illustrates the particle size distribution of the metal particles used. Their specific weights, as well as the temperature they achieved (peak and average) when situated 2 cm beneath a coil under 100 A magnetic induction, are shown in Table 2. Since 20 ºC was the room temperature, the values in Table 2 indicated that GSBP was almost completely insensitive to magnetic induction.derr

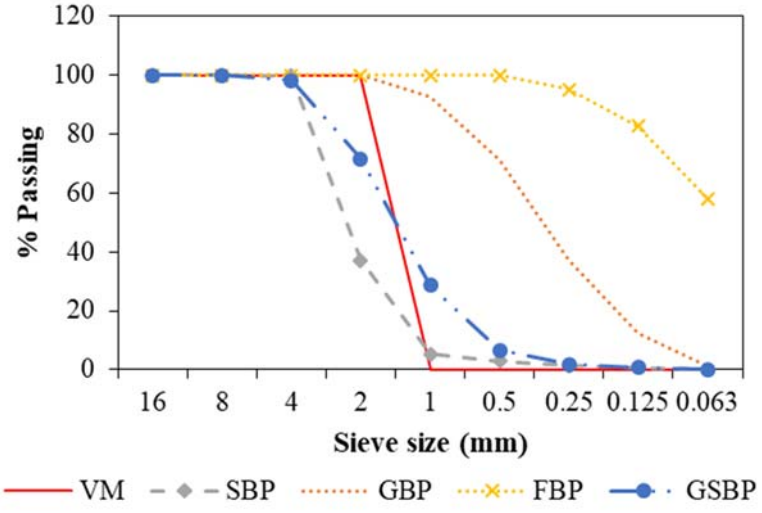

Figure 5. Particle size distribution of the metal particles tested

Table 2. Specific weight and temperature achieved by the metal particles tested

Metal particle	Specific weight (Kg/m3)	Heating test	
		Peak T[a] (ºC)	Average T[a] (ºC)
VM	7.850	79.8	59.4
SBP	7.465	87.4	45.4
GBP	7.639	73.8	39.2
FBP	3.585	53.2	32.0
GSBP	2.875	20.0	20.0

After this initial characterization, the metal particles were incorporated into the manufacture of 5 different mixtures. The first two mixtures consisted of the addition of a single heating inductor to the aggregates and the bitumen: VM and GBP. The third and fifth mixtures combined GBP with two by-products having a limited or almost inexistent reaction to magnetic induction, such as FBP and GSBP, whilst the fourth mixture emerged from the coupling of SBP and FBP. To ease the nomenclature of these mixtures they were named as VM, SB1, SB2, JB1 and JB2, such that SBx means that a single metal inductor was added and JBx indicates that two by-products were jointly included. The dosage of the five experimental mixtures is shown in Table 3 as the difference between each sieve passing value and the spindle centre of the dosage of an AC-16 mixture, which was taken as a reference as explained in Figure 2.

Table 3. Dosage of the experimental mixtures in comparison with the spindle center of that corresponding to dense asphalt concrete (AC-16)

Mixture	Sieve size (mm)									
	22.0	16	8	4	2	1	0.5	0.25	0.13	0.063
AC-16*	100.0	95.0	67.5	42.5	31.0	23.5	16.0	11.0	8.0	5.0
VM	0	+5.0	+2.8	+1.8	+3.1	-2.1	-1.7	-0.6		+1.6
SB	0	+5.0	+2.9	+1.9	+1.3	+1.3	+0.7	+0.3	+0.4	+1.0
JB1	0	+5.0	+2.4	+1.5	+1.1	+1.1	+0.6	+0.3	+0.3	+0.5
JB2	0	+5.0	+1.7	+1.1	+0.0	-1.2	-1.0	+0.3	+0.7	+1.1
JB3	0	+5.0	+3.4	+2.1	+1.3	+1.4	+0.8	-0.4	+0.4	+1.9

* Values corresponding to the spindle cente

All the experimental mixtures were subjected to the break-heal-break test as described in the methodology. Hence, the loads resisted before and after healing by each mixture under different pairs of induction intensity and time were recorded, in order to facilitate their comparison. The VM specimens were initially tested with intensities of between 400 A and 600 A and times above 120 s. For instance, the specimens tested for 240 s at 500 A reached a peak HR of 73%; nevertheless, they achieved temperatures (above 150 ºC), which is not admissible to ensure the absence of changes in the bitumen. Thus, intensities were lowered to 400 A and 300 A, leading to healing ratios of up to 45 % and 47 % when heated during 120 s and 240 s, respectively.

Intensities between 300 A and 400 A were not sufficient to achieve good healing ratios in the SB mixture, to the extent that the specimens tested during 240 s at 300 A only reached values of HR of 7 %. Higher HR values started when applying 500 A during 240 s (about 47 %). In this case, the surface temperature of the specimens was about 90 ºC, which was considered a suitable value to soften the bitumen and let it flow to close any crack within the specimens. Two more groups of SB specimens were tested by increasing the intensity to 600 A with times of 240 s and 300 s. These two groups provided healing ratios of 47 % and 55 %, respectively, without exceeding a surface temperature of 130 ºC.

Again, currents of 300 A and 400 A were not enough to sufficiently heat and, therefore, heal the JB1 mixtures. The coupling of a current of 500 A with healing times between 180 s and 300 s yielded higher healing ratios, whilst the highest HR (31%) corresponded to a combination of 240 s and 600 A. Still, the results were not as good as those achieved in other mixtures. The lower amount of GBP by-products in JB1 in relation to SB explained why it resulted in an inferior healing performance. Furthermore, JB1 also contained FBP, which was found to be insensitive to magnetic induction (Figure 5).

To reduce the risk of overheating the JB2 specimens, the asphalt mixtures containing SBP and FBP were tested at currents of 400 A and 500 A and healing times between 120 s and 180 s. The best performance was obtained by combining 180 s and 400 A, whereby the values of HR reached a maximum of 65 %. In general, the results of JB2 showed higher variability than other mixtures. This is probably due to the SBP particle size, which is substantially bigger that those of the other by-products tested and can result in either less homogeneous mixtures or boost the loss of aggregates when breaking the specimens.

The final mixture, JB3, contained two by-products: GBP and GSBP. Taking into account that GSBP barely contributed to the heating of the mixture when applying magnetic induction, these specimens were tested using the maximum current intensity of 600 A and varying healing times between 240 s and 300 s. The highest values of HR reached were about 60%, suggesting that the longer the test, the higher the healing ratio when intensity remained steady.

3.2. Statistical modelling

3.2.1. Cluster Analysis

The characterization and dosages conducted in laboratory enabled the determination of the specific weight and content of the additives included in the mixtures as heating inductors. These were the variables used for the cluster analysis, as representatives of the intrinsic properties of the particles used. In mixtures with more than one single additive, specific weight was calculated as the weighted average of the individual values corresponding to each particle type, whilst content was computed as their sum.

As a result, the following pairs of values [specific weight (kg/m^3), content (%)] were obtained for the inductors included in the 5 asphalt mixtures under evaluation: [7.850, 5.0] (VM), [7.639, 4.4] (SB), [6.312, 5.5] (JB1), [6.041, 7.9] (JB2) and [5.405, 11.3] (JB3). The application of Eqs. (2) and (3) according to these values yielded the dendrogram depicted in Figure 6. Although the density and amount of the metal particles added to the mixtures were different in all cases, their dosage was adjusted to be coincident and fit the gradation of an AC-16 specimen, thus making them comparable to each other. Moreover, having a variety of combinations of specific weight and content was a requirement for building prediction models to optimize the valorization of by-products included in asphalt mixtures with self-healing purposes, which was the ultimate objective of this research.

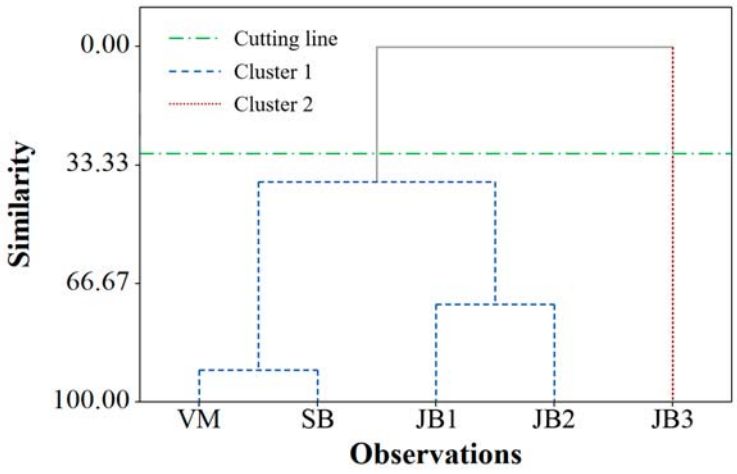

Figure 6. Dendrogram indicating the clustering options to group the experimental mixtures according to their similarity

The clustering algorithm began by yielding 5 groups, one per mixture, and then continued by producing increasingly heterogeneous conglomerates. Hence, the second possible cut involved 4 groups, whereby the only cluster formed included VM and SB constituents, whose content and specific weight are similar. The next step corresponded to the grouping of JB1 and JB2, leaving JB3 in isolation. Finally, the last meaningful level clustered all the mixtures except JB3. Since grouping definition is affected by the step where the values change more abruptly, the cutting line was drawn to result in 2 clusters, as represented in Figure 6.

Due to the low representativeness of the second cluster, JB3 was removed from subsequent steps. This line of action was consistent with the magnetic and thermal response observed in the particles used as inductors in this mixture, since GSBP was found to be very limited in those terms and made the application of high values of time and intensity necessary. Still, the low resistance of this by-product led to misleading results of HR. An

alternative path consisting of considering only GBP in JB3 for modelling would not provide added value to the final outcome of the study, reaffirming the decision to exclude this mixture for prediction purposes.

The values of HR obtained for the remaining mixtures were arranged according to the time and current intensity used. As the same combinations of values were applied to the same specimens repeatedly until the results converged using Eq. (1), the data used from this point were the mean values of HR obtained from such replicates, as specified in Table 4. To ensure the validity of subsequent prediction models, one randomly chosen sample of each mixture was excluded from regression analysis for testing purposes. Under the premise of using different values of heating time and intensity depending on the purity of the metal particles, the healing ratios obtained were in the same order of magnitude in most cases. The main exception to this line was found in SB_3, which only recovered 6.9% of its initial resistance after the process due to its reduced content of metal particles and the low intensity applied.

Table 4. Training and testing combinations of predictors used to model the healing ratio (***HR***) of asphalt mixtures through multiple regression analysis

Purpose	Mixture	Metal particles		Time (s)	Intensity (A)	*HR* (%)
		Specific weight (kg/m^3)	Content (%)			
Training	VM_1	7.850	5.0	120	400	28.331
Training	VM_2	7.850	5.0	240	500	67.039
Training	VM_3	7.850	5.0	240	300	45.850
Testing	VM_4	7.850	5.0	120	500	40.984
Training	SB_1	7.639	4.4	240	600	47.709
Training	SB_2	7.639	4.4	300	600	57.822
Training	SB_3	7.639	4.4	240	300	6.914
Testing	SB_4	7.639	4.4	240	500	42.041
Training	JB1_1	6.312	5.5	180	500	15.846
Training	JB1_2	6.312	5.5	120	600	14.976
Training	JB1_3	6.312	5.5	300	500	38.423
Testing	JB1_4	6.312	5.5	240	500	27.243
Training	JB2_1	6.041	7.9	240	300	38.556
Training	JB2_2	6.041	7.9	180	400	57.548
Training	JB2_3	6.041	7.9	120	400	36.300
Testing	JB2_4	6.041	7.9	120	500	40.789

3.2.2. Multiple Regression Analysis

The values of specific weight, content, time and intensity compiled in Table 4 were used as predictors to model HR, which performed as response, through multiple regression analysis. The use of Eq. (4) led to obtain the model summarized in Table 5, which

demonstrated that the interactive effect of specific weight (X_1) with the remaining predictors (X_2, X_3 and X_4) was statistically significant (p-values < 0.05 in all cases) and explained 90 % (R^2) of the variability of the HR values around its mean. The model was determined using the stepwise method, whose working principle consists of systematically adding the most significant term or removing the least significant term during each step. The results of this procedure indicated that the most efficient model to fit HR was based on the three interactions referred above, such that adding, replacing or removing any term, either single variables or interactions, did not improve its quality.

All the coefficients associated with these terms were positive, which was logical according to the physical relationships between the predictors and the response. Hence, the percentage of resistance recovered after healing was proportional to the purity of the metal particles and their content in the mixture, which favoured the fluency of the bitumen through the rapid heating of the mixtures. The healing ratios also increased as long as the values of time and the intensity applied during the process were higher, boosting the heating of the inductors. Furthermore, the p-value of the F-tests for the regression term was also below the significance level, indicating that the model built provided a better fit than the intercept-only model.

Table 5. Summary of the multiple regression model built for estimating the healing ratio (***HR***) of asphalt mixtures

S	R^2	Adj. R^2	PRESS	Pred. R^2
7.025	0.90	0.86	962.164	0.75
Term	**Coef**	**F-Value**	**p-value**	**VIF**
Regression	-	23.40	0.000	-
Constant	-195.6	-	0.000	-
$X_1 * X_2$	3.739	53.65	0.000	1.95
$X_1 * X_3$	0.025	29.43	0.001	1.28
$X_1 * X_4$	0.017	30.25	0.001	1.73

The value of Adj. R^2 reached (0.86) suggested that the accuracy of the model was not compromised by the number of predictors used, since it did not differ much from the standard R^2. This was corroborated by the Variance Inflation Factors (VIF), which were very close to the lower bound of this measure (1) for all predictors, suggesting that multicollinearity was not an issue. Although the Pred. R^2 slightly decreased in comparison with these two coefficients, it was high enough to validate it for making new predictions. The standard error of the regression (S) was strongly affected by JB2, which was responsible for almost half of the distance between the values measured in laboratory and the regression line. This was mainly attributable to the size of SBP and its combination FBP in large quantities (Table 4), which hindered the modelling of this mixture and led it to reach the highest values of HR under all the combinations of time and intensity, as demonstrated in the contour plots in Figure 7. On the contrary, the limited purity and amounts

472 of by-products contained in JB1 explained its poor healing performance in comparison
473 with the remaining mixtures (Figure 7(c)).
474

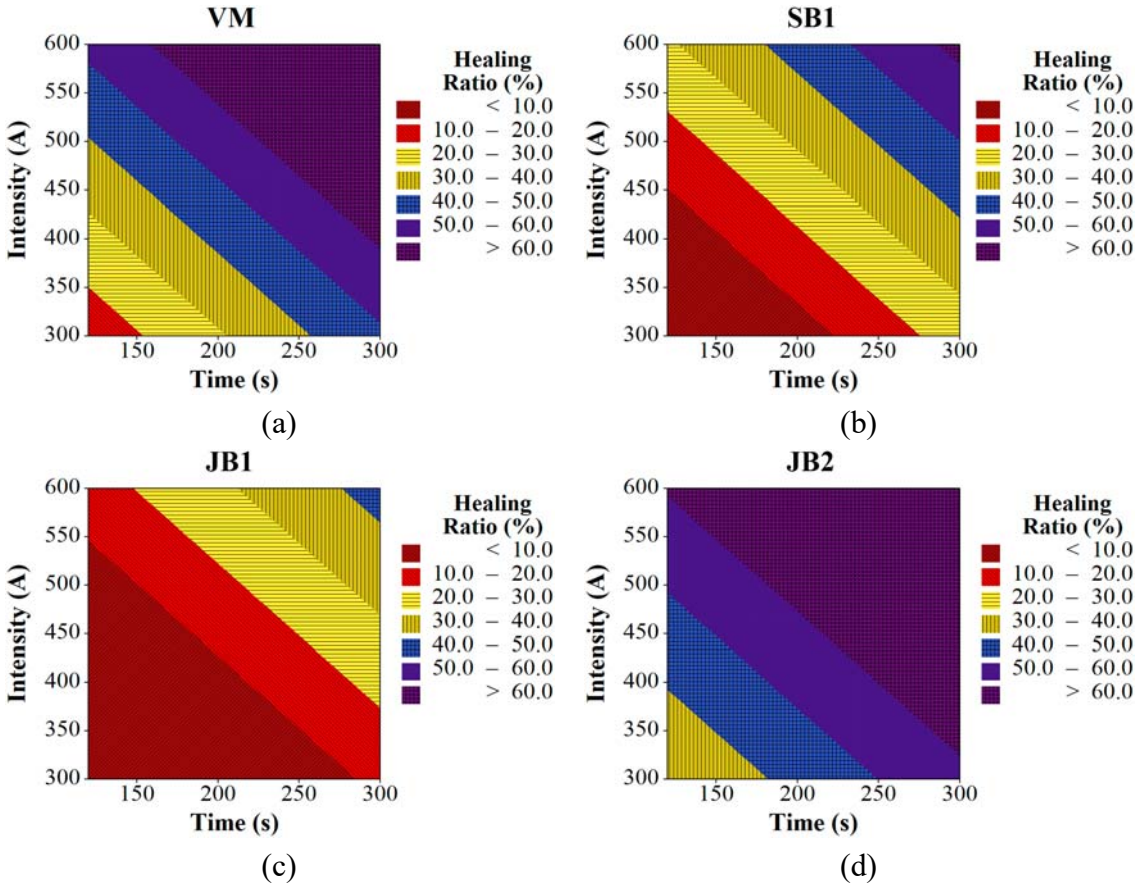

475 **Figure 7.** Contour maps representing the relationship between the values time (s) and intensity (A) with
476 the healing ratio (***HR***) achieved by asphalt mixtures (a) VM (b) SB (c) JB1 (d) JB2
477

478 The reliability of the regression model built was first checked in analytical terms, as
479 shown in Table 6. The Shapiro-Wilk and Levene's tests yielded p-values above the sig-
480 nificance level (0.05), guaranteeing the normality and homoscedasticity of residuals.
481 Their independence was checked through the comparison of the Durbin-Watson statistic
482 (D) with the lower (D_L) and upper (D_U) bounds established by Savin and White (1977)
483 [38], such that $(4 - D) > D_U$ indicates an absence of serial correlation, $D < D_L$ suggests
484 a positive correlation and $D_L < D < D_U$ involves that the test is inconclusive. For a sam-
485 ple size of 12 (Table 4) and a number of terms equal to 3 (Table 5), D_L and D_U are 0.812
486 and 1.579, respectively. Since $(4 - D) = 1.467$, the test was found to be inconclusive.
487

488 **Table 6.** Analytical verification of the assumptions involving the residuals of multiple regression analysis

Normality		**Homoscedasticity**		**Independence**
Shapiro-Wilk	**p-value**	**Levene**	**p-value**	**Durbin-Watson**
0.970	0.915	0140	0.931	2.533

489

490 To further ensure the robustness of the model summarized in Table 5, the assumptions
491 concerning its residuals were also verified graphically, as illustrated in Figure 8. The re-
492 semblance of the residuals to the reference line of the quantile-quantile (Q-Q) plot, as

well as the approximate bell-shape of the histogram, confirmed that the assumption of normality was met. The unbiased distribution of the residuals in the versus fits plot also ensured the homoscedasticity of the model. Finally, the lack of clear patterns and the random location of the residuals around the reference line in the versus order graph indicated that they were not correlated to each other, which enabled assuming their independence too.

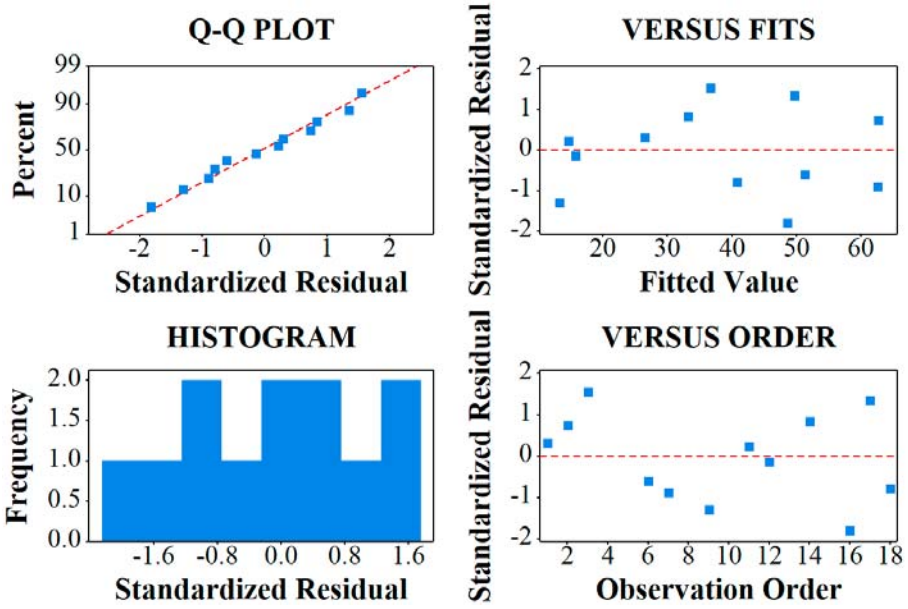

Figure 8. Residual plots used to test the assumptions of multiple regression analysis graphically

As a final step to prove the validity of the regression analysis conducted, the model summarized in Table 5 was used to estimate the healing capacity corresponding to the specimens reserved for testing, as indicated in Table 4. Figure 9 illustrates the fit between the values of *HR* measured in laboratory and the regression model. The results proved to be very accurate for the VM, SB and JB1 mixtures, to the extent that the errors between measured and predicted values were less than half *S* in all cases (Table 5). However, the estimate for the JB2 mixture resulted in an error of 10.016, which ratified the singularity of this mixture, as a result of its uneven combination of low specific weight and high content of by-products.

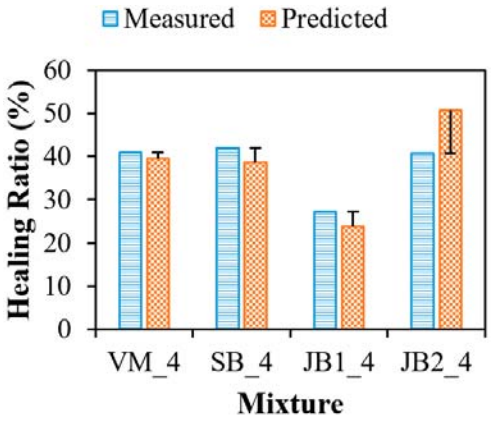

Figure 9. Fit between the values of healing ratio (***HR***) measured in laboratory and predicted through multiple regression analysis for the specimens reserved for testing

3.2.3. Response Optimization

Based on the multiple regression model built in Table 5, the application of the response optimization framework enabled the calculation of the minimum amount of time and resources required to achieve *HR* targeted values. Figure 10 depicts the working principle of this approach, indicating the extent to which changes in the variables used as predictors produced variations in the healing ratio. Hence, the variations derived from the displacement of the vertical lines associated with the predictors with respect to the horizontal axis can be combined to reach desired healing ratios. This is exemplified for a mixture containing 5.5 % of GBP and subject to induction during 200 s at 600 A, which resulted in a value of *HR* of 49.8 %.

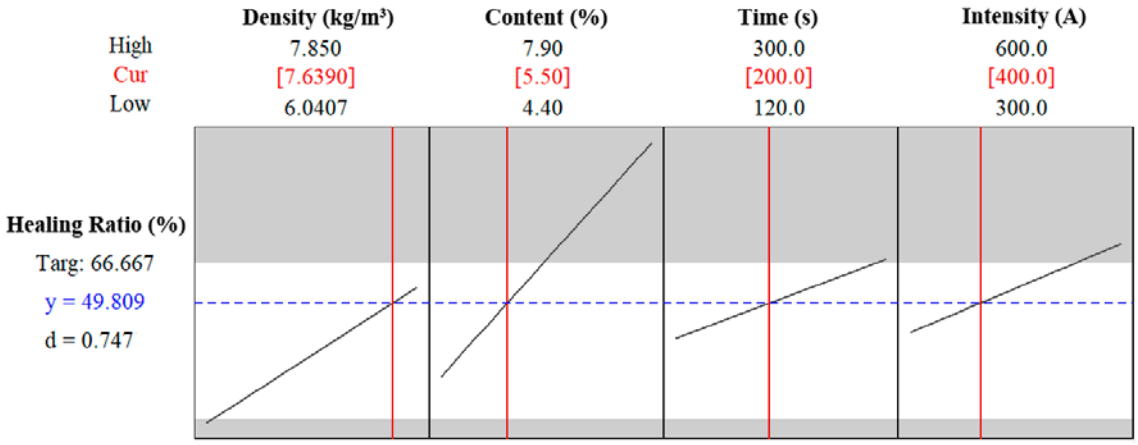

Figure 10. Optimization plot produced to target a healing ratio (***HR***) of 66.667 % by changing the values taken by the predictors

In this case, a healing ratio of 66.7 % was set as a target, representing a recovery of two thirds of the original resistance of asphalt mixtures after breaking. This value was considered to be representative for a reasonable degree of healing capacity under real conditions. Since the underlying objectives sought were saving resources and be as time-

efficient as possible, intensity was a restricted parameter established according to the heating susceptibility of the metal particles. Therefore, this parameter was set at 500 A in VM and JBP1, which proved to be more likely to produce alterations in the bitumen, and was increased to 600 A for SBP1 and SBP2. The implementation of the desirability function synthetized in Eq. (5) according to these conditions yielded the results compiled in Table 7.

Table 7. Optimized values of content (%) and time (s) obtained for the resource efficiency and quickness scenarios using the desirability function approach

Mixture	Objective	Content (%)	Time (s)	Intensity (A)	Healing Ratio (%)	$\delta_i(\hat{Y}_i)$
VM	Resource efficiency	4.760	297.119	500.000	66.667	1.000
	Quickness	5.926	120.000	500.000	66.667	1.000
SBP1	Resource efficiency	4.563	297.006	600.000	66.667	1.000
	Quickness	5.728	120.000	600.000	66.667	1.000
SBP2	Resource efficiency	6.474	300.000	600.000	66.667	1.000
	Quickness	7.658	120.000	600.000	66.667	1.000
JBP1	Resource efficiency	7.418	300.000	500.000	66.667	1.000
	Quickness	7.900	120.001	500.000	50.805	0.735

Overall, all the mixtures were found to be capable of achieving the target established ($\delta_i(\hat{Y}_i) = 1$), except JBP1 for the quickness scenario, which resulted in a desirability of 0.735. This low value of $\delta_i(\hat{Y}_i)$ was due to the content of the metal particles used to manufacture this mixture, which was the upper bound taken by the optimization problem for this variable. Reaching a value of $\delta_i(\hat{Y}_i) = 1$ in this scenario would involve increasing the by-products to approx. 10 % ; however, this course of action may result in an excessively dense asphalt mixture, which would cause transportation and installation problems.

Otherwise, the remaining mixtures reached the value of HR sought under both scenarios. Beyond the limitations of the regression model (Table 5), the values of content and time (Table 7) show how the self-healing of asphalt mixtures can be optimized in terms of either resource or time efficiency. In particular, the first course of action would be to maximize the valorization of metal wastes in the road industry, where the construction and maintenance of pavements traditionally involve large amounts of raw material. However, since the metal particle contents yielded by the optimization process differed from those used to manufacture the specimens in laboratory to resemble an AC-16 dense asphalt mixture (Figure 2), the practical application of these values would require redesigning their dosage, in order to ensure that they meet the mechanical and technical parameters required for their implementation.

4. Conclusions

This study was concerned with the statistical modelling of the self-healing capacity of asphalt mixtures containing different combinations of metal particles, focusing on the use of industrial metal by-products to reduce economic cost and environmental impacts of road materials. A methodology integrating cluster algorithms, multiple regression analysis and response optimization was designed, applied and validated using the results obtained in laboratory regarding the healing potential of five experimental asphalt mixtures heated through magnetic induction. The analysis of these results led to the following conclusions:

- The experimental tests highlighted the suitability of the metallic by-products used as heating inductors in the self-healing process of asphalt mixtures. The only exception to this trend were the green foundry slags, whose thermal and magnetic response was almost null. In general, the values of heating time and intensity required by the experimental mixtures were higher due to the lower purity of the by-products, although the steel shot wastes from sandblasting resulted in healing ratios similar to those of the control specimens with virgin metal particles.
- In line with the inferences extracted from the laboratory results, cluster analysis led to discard the mixture type containing green slags, due to its almost null heating potential and high fragility. The regression model built to replicate the laboratory results for the four remaining mixtures reached high coefficients of determination and met all the assumptions regarding its residuals, guaranteeing its reliability to make new predictions. In fact, the application of the model to the specimens excluded from the analysis for testing purposes yielded estimates in the order of magnitude of the standard error of the regression, which further corroborated its validity.
- The desirability function approach used for response optimization showed that the amount of metal particles to include in the mixtures and the time of magnetic induction required to achieve targeted healing ratios. This step was intended to increase the viability of the self-healing of asphalt mixtures. On the one hand, it can help to maximize the recycling of industrial by-products as a valuable resource in asphalt design and road conservation. On the other hand, it can also limit the traffic disruptions associated with conventional road maintenance practices by designing asphalt mixtures that minimize the time required to apply magnetic induction.

Although the results produced in this study proved to be valid and meaningful, further work is needed. Future work should focus on testing the proposed framework using more specimens with different values of specific weight and content of metal particles, as well as new asphalt mixture dosages to verify how generalizable the optimized results are. In this vein, another area of research to develop in the future concerns the incorporation of additional mechanical tests conducted in laboratory into the statistical modelling, in order to provide a more comprehensive characterization of the experimental behaviour of self-healing asphalt mixtures.

Acknowledgments

This paper was possible thanks to the research project SIMA+ (Ref. BIA2016-77372-R), financed by the Spanish Ministry of Economy and Competitiveness with funds from the State General Budget (PGE) and the European Regional Development Fund (ERDF). Marta Vila-Cortavitarte would also like to express her gratitude to the Spanish Ministry of Economy and Competitiveness for funding her investigations at the University of Cantabria through a Researcher Formation Fellowship (Ref. BES-2017-079882).

References

[1] L.F. Walubita, E. Mahmoud, S.I. Lee, G. Carrasco, J.J. Komba, L. Fuentes, T.P. Nyamuhokya, Use of grid reinforcement in HMA overlays – A Texas field case study of highway US 59 in Atlanta District, Constr. Build. Mater. 213 (2019) 325–336. doi:10.1016/J.CONBUILDMAT.2019.04.072.

[2] Á. García, E. Schlangen, M. van de Ven, Q. Liu, Electrical conductivity of asphalt mortar containing conductive fibers and fillers, Constr. Build. Mater. 23 (2009) 3175–3181. doi:10.1016/J.CONBUILDMAT.2009.06.014.

[3] Q. Liu, A. García, E. Schlangen, M.V.D. Ven, Induction healing of asphalt mastic and porous asphalt concrete, Constr. Build. Mater. 25 (2011) 3746–3752. doi:10.1016/j.conbuildmat.2011.04.016.

[4] A. Tabaković, D. O'Prey, D. McKenna, D. Woodward, Microwave self-healing technology as airfield porous asphalt friction course repair and maintenance system, Case Stud. Constr. Mater. 10 (2019) e00233. doi:10.1016/J.CSCM.2019.E00233.

[5] Argusmedia, Argus Asphalt Report, (2014). https://es.scribd.com/document/251813947/Bitumen-Report-Argus-Asphalt.

[6] J. Yin, W. Wu, Utilization of waste nylon wire in stone matrix asphalt mixtures, Waste Manag. 78 (2018) 948–954. doi:10.1016/j.wasman.2018.06.055.

[7] M.C. Zanetti, S. Fiore, B. Ruffino, E. Santagata, D. Dalmazzo, M. Lanotte, Characterization of crumb rubber from end-of-life tyres for paving applications, Waste Manag. 45 (2015) 161–170. doi:10.1016/j.wasman.2015.05.003.

[8] J. Choudhary, B. Kumar, A. Gupta, Application of waste materials as fillers in bituminous mixes, Waste Manag. 78 (2018) 417–425. doi:10.1016/j.wasman.2018.06.009.

[9] M.A. Franesqui, J. Yepes, C. García-González, Top-down cracking self-healing of asphalt pavements with steel filler from industrial waste applying microwaves, Constr. Build. Mater. 149 (2017) 612–620. doi:10.1016/j.conbuildmat.2017.05.161.

[10] J. Norambuena-Contreras, A. Gonzalez, J.L. Concha, I. Gonzalez-Torre, E. Schlangen, Effect of metallic waste addition on the electrical, thermophysical and microwave crack-healing properties of asphalt mixtures, Constr. Build. Mater. 187 (2018) 1039–1050. doi:10.1016/j.conbuildmat.2018.08.053.

[11] M. Vila-Cortavitarte, D. Jato-Espino, D. Castro-Fresno, M.Á. Calzada-Pérez, Self-healing capacity of asphalt mixtures including by-products both as aggregates and heating inductors, Materials (Basel). 11 (2018) 800. doi:10.3390/ma11050800.

[12] A. García, J. Norambuena-Contreras, M.N. Partl, Experimental evaluation of dense

asphalt concrete properties for induction heating purposes, Constr. Build. Mater. 46 (2013) 48–54. doi:10.1016/j.conbuildmat.2013.04.030.

[13] A. Menozzi, A. Garcia, M.N. Partl, G. Tebaldi, P. Schuetz, Induction healing of fatigue damage in asphalt test samples, Constr. Build. Mater. 74 (2015) 162–168. doi:10.1016/j.conbuildmat.2014.10.034.

[14] L.F. Walubita, Comparison of fatigue analysis approaches for predicting fatigue lives of hot-mix asphalt concrete (HMAC) mixtures, (2006). https://oaktrust.library.tamu.edu/handle/1969.1/3898 (accessed June 25, 2019).

[15] Q. Liu, E. Schlangen, Á. García, M. van de Ven, Induction heating of electrically conductive porous asphalt concrete, Constr. Build. Mater. 24 (2010) 1207–1213. doi:10.1016/j.conbuildmat.2009.12.019.

[16] A. García, J. Norambuena-Contreras, M. Bueno, M.N. Partl, Single and multiple healing of porous and dense asphalt concrete, J. Intell. Mater. Syst. Struct. 26 (2015) 425–433. doi:10.1177/1045389X14529029.

[17] X. Zhu, Y. Cai, S. Zhong, J. Zhu, H. Zhao, Self-healing efficiency of ferrite-filled asphalt mixture after microwave irradiation, Constr. Build. Mater. 141 (2017) 12–22. doi:10.1016/j.conbuildmat.2017.02.145.

[18] J. Qiu, M.F.C. Ven, E. Schlangen, S. Wu, A.A.A. Molenaar, Cracking and Healing Modelling of Asphalt Mixtures, in: 7th RILEM Int. Conf. Crack. Pavements, 2012. doi:10.1007/978-94-007-4566-7_108.

[19] V. Magnanimo, H.L. Huerne, S. Luding, Asphalt Durability and Self-healing Modelling with Discrete Particles Approach, in: 7th RILEM Int. Conf. Crack. Pavements, 2012. doi:10.1007/978-94-007-4566-7_105.

[20] L.F. Walubita, J. Hoeffner, T. Scullion, T.A.T. Institute, U. of T. at S. Antonio, New Generation Mix-Designs: Laboratory-Field Testing and Modifications to Texas HMA Mix-Design Procedures, (2012). https://rosap.ntl.bts.gov/view/dot/26116 (accessed June 25, 2019).

[21] X. Yang, Q. Dai, Z. You, Z. Wang, Integrated Experimental-Numerical Approach for Estimating Asphalt Mixture Induction Healing Level through Discrete Element Modeling of a Single-Edge Notched Beam Test, J. Mater. Civ. Eng. (2014). doi:10.1061/(asce)mt.1943-5533.0001231.

[22] V. Chowdary, J. Murali Krishnan, A thermodynamic framework for modelling healing of asphalt mixtures, Int. J. Pavement Res. Technol. (2010).

[23] X. Luo, R. Luo, R.L. Lytton, Mechanistic modeling of healing in asphalt mixtures using internal stress, Int. J. Solids Struct. (2015). doi:10.1016/j.ijsolstr.2015.01.028.

[24] E. Levenberg, Modelling asphalt concrete viscoelasticity with damage and healing, Int. J. Pavement Eng. (2017). doi:10.1080/10298436.2015.1066004.

[25] UNE, EN 933-1:2012, (2012). https://www.une.org/encuentra-tu-norma/busca-tu-norma/norma/?c=N0049638 (accessed August 7, 2018).

[26] UNE, Norma UNE-EN 1097-6:2014, (2014). https://www.une.org/encuentra-tu-norma/busca-tu-norma/norma/?c=N0052839 (accessed November 21, 2018).

[27] R.C. Tryon, Cluster Analysis: Correlation Profile and Orthometric (factor) Analysis for the Isolation of Unities in Mind and Personality, Edwards Brothers Malloy, Ann Arbor (U.S.), 1939.

[28] O. Maimon, L. Rokach, Data Mining and Knowledge Discovery Handbook, Springer, Berlin (Germany), 2005.

[29] E.A. Mooi, M. Sarstedt, A concise guide to market research: the process, data, and methods using IBM SPSS Statistics, Springer, Heilderberg (Germany), 2011.

[30] N.C. Jain, A. Indrayan, L.R. Goel, Monte Carlo comparison of six hierarchical

clustering methods on random data, Pattern Recognit. 19 (1986) 95–99. doi:10.1016/0031-3203(86)90038-5.
[31] R.A. Fisher, Statistical Methods for Research Workers, in: S. Kotz, N.L. Johnson (Eds.), Break. Stat. Methodol. Distrib., Springer, New York (U.S.), 1992: pp. 66–70. doi:10.1007/978-1-4612-4380-9_6.
[32] J. Zolgharnein, A. Shahmoradi, Characterization of Sorption Isotherms, Kinetic Models, and Multivariate Approach for Optimization of Hg(II) Adsorption onto *Fraxinus* Tree Leaves, J. Chem. Eng. Data. 55 (2010) 5040–5049. doi:10.1021/je1006218.
[33] J.L. Gastwirth, Y.R. Gel, W. Miao, The Impact of Levene's Test of Equality of Variances on Statistical Theory and Practice, Stat. Sci. 24 (2009) 343–360. doi:10.1214/09-STS301.
[34] J. Durbin, G.S. Watson, Testing for serial correlation in least squares regression. I., Biometrika. 37 (1950) 409–428. doi:10.1093/biomet/37.3-4.409.
[35] J. Durbin, G.S. Watson, Testing for serial correlation in least squares regression. II., Biometrika. 38 (1951) 159–178.
[36] J.W. Osborne, E. Waters, Four assumptions of multiple regression that researchers should always test, Pract. Assessment, Res. Eval. 8 (2003).
[37] G. Derringer, R. Suich, Simultaneous Optimization of Several Response Variables, J. Qual. Technol. 12 (1980) 214–219. doi:10.1080/00224065.1980.11980968.
[38] N.E. Savin, K.J. White, The Durbin-Watson Test for Serial Correlation with Extreme Sample Sizes or Many Regressors, Econometrica. 45 (1977) 1989–1996.